



Transcriptomic Analysis of *Mecp2* Mutant Mice Reveals Differentially Expressed Genes and Altered Mechanisms in Both Blood and Brain

Albert Sanfeliu¹, Karsten Hokamp², Michael Gill¹ and Daniela Tropea^{1,3*}

¹Neuropsychiatric Genetics, Department of Psychiatry, School of Medicine, Trinity Translational Medicine Institute, St James Hospital, Dublin, Ireland, ²Department of Genetics, School of Genetics and Microbiology, Smurfit Institute of Genetics, Trinity College Dublin, Dublin, Ireland, ³Department of Psychiatry, School of Medicine, Trinity College Institute for Neuroscience, Trinity College Dublin, Dublin, Ireland

OPEN ACCESS

Edited by:

Yuri Bozzi,
University of Trento,
Italy

Reviewed by:

Janine M. LaSalle,
University of California, Davis,
United States
Maurizio Giustetto,
University of Turin,
Italy

*Correspondence:

Daniela Tropea
tropead@tcd.ie

Specialty section:

This article was submitted to
Child and Adolescent Psychiatry,
a section of the journal
Frontiers in Psychiatry

Received: 07 March 2019

Accepted: 11 April 2019

Published: 29 April 2019

Citation:

Sanfeliu A, Hokamp K, Gill M and
Tropea D (2019) Transcriptomic
Analysis of *Mecp2* Mutant Mice
Reveals Differentially Expressed
Genes and Altered Mechanisms in
Both Blood and Brain.
Front. Psychiatry 10:278.
doi: 10.3389/fpsy.2019.00278

Rett syndrome is a rare neuropsychiatric disorder with a wide symptomatology including impaired communication and movement, cardio-respiratory abnormalities, and seizures. The clinical presentation is typically associated to mutations in the gene coding for the methyl-CpG-binding protein 2 (*MECP2*), which is a transcription factor. The gene is ubiquitously present in all the cells of the organism with a peak of expression in neurons. For this reason, most of the studies in Rett models have been performed in brain. However, some of the symptoms of Rett are linked to the peripheral expression of *MECP2*, suggesting that the effects of the mutations affect gene expression levels in tissues other than the brain. We used RNA sequencing in *Mecp2* mutant mice and matched controls, to identify common genes and pathways differentially regulated across different tissues. We performed our study in brain and peripheral blood, and we identified differentially expressed genes (DEGs) and pathways in each tissue. Then, we compared the genes and mechanisms identified in each preparation. We found that some genes and molecular pathways that are differentially expressed in brain are also differentially expressed in blood of *Mecp2* mutant mice at a symptomatic—but not presymptomatic—stage. This is the case for the gene *Ube2v1*, linked to ubiquitination system, and *Serpin1*, involved in complement and coagulation cascades. Analysis of biological functions in the brain shows the enrichment of mechanisms correlated to circadian rhythms, while in the blood are enriched the mechanisms of response to stimulus—including immune response. Some mechanisms are enriched in both preparations, such as lipid metabolism and response to stress. These results suggest that analysis of peripheral blood can reveal ubiquitous altered molecular mechanisms of Rett and have applications in diagnosis and treatments' assessments.

Keywords: Rett syndrome, methyl-CpG-binding protein 2, gene expression, transcriptomics, cerebellum, blood

INTRODUCTION

Rett syndrome (RTT) is a rare neurological disease, affecting approximately 1 in every 10,000 live female births. Approximately 95% of RTT cases present with mutations in the *MECP2* gene, which is located in the long arm of the X chromosome (1). Its genomic location explains why the majority of patients are females. Females can compensate for loss of *MECP2* function with an extra intact

copy on the homologous X chromosome, but this is not the case for males. Consequently, males have a severe phenotype and represent less than 1% of RTT patients.

The symptoms manifest after a period of apparent normality, corresponding to the first 6–18 months of life. After this stage, patients present neurological features (microcephaly, seizure), motor disability (ataxia, loss of purposeful hand use, stereotyped hand movements, loss of the ability to walk, hypotonia), social impairment (loss of speech, unresponsiveness to social cues, lack of emotional expression), and autonomic complications (respiratory anomalies, cardiac dysfunction, constipation) (2). The symptoms and their severity can be variable from one patient to another. One of the reasons for this variability is thought to be skewed X-inactivation, as patients with an X-inactivation biased to the nonmutated copy of *MECP2* have shown little to no symptoms (3).

The strong association between *MECP2* mutations and the disease has prompted the generation of mutant mice, which present specific mutations in *Mecp2* or a lack of its expression (4–10). These mice show signs that resemble the symptoms in patients; hence, they are considered valuable models for shedding light on the molecular mechanisms underlying RTT (4, 5).

MECP2 encodes for methyl-CpG-binding protein 2 (MeCP2), a chromatin binding protein (11) that is expressed ubiquitously in the body with major expression in the central nervous system (CNS). As MeCP2 was first postulated as a transcriptional repressor, several groups used the mouse models to study gene expression changes (12–14). These studies have revealed that MeCP2 can both upregulate and downregulate gene expression, and that gene expression changes are specific to different brain areas and cell types (12–14).

Although *MECP2* is highly expressed in the brain, it is also present in several other tissues/organs, and a recent mouse model showed that a small portion of symptoms are still present when *Mecp2* is exclusively expressed in the CNS but not in the rest of the body (15), supporting the possibility that molecular signatures of dysfunctions in RTT may be present in peripheral tissues, and they are possibly linked to changes in the brain.

In our study, we used RNA sequencing to compare the differential gene expression in brain and in blood in a mouse

model of RTT. This analysis reveals associations between genes expressed in the two tissues and has important applications in the detection of peripheral biomarkers for Rett syndrome.

RESULTS

MeCP2 Protein Expression Levels Are High in Mouse Cerebellum at 7 Weeks of Age

In the brain, the expression of *Mecp2* is dynamically modulated during development (16, 17). Additionally, *Mecp2* expression can differ between brain areas (15), as well as the genes that *Mecp2* regulates (13). For these reasons, we understand that to perform a transcriptomic analysis, it is necessary to use a specific brain area, and that the area should ideally have high levels of MeCP2 expression at the developmental stage in which the study is conducted.

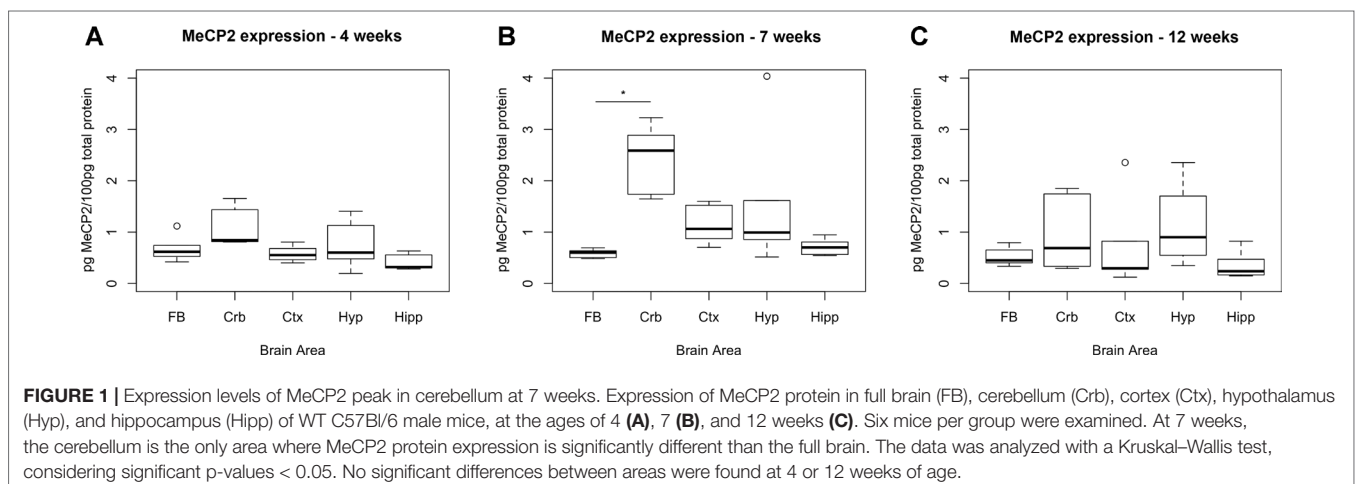
To identify the ideal brain region for the developmental stage of our study (i.e., 7 weeks, when symptoms are advanced in the *Mecp2*-null male), we measured the temporal expression of MeCP2 protein in wild-type (WT) C57Bl/6 male mice in different brain areas (cortex, cerebellum, hippocampus, and hypothalamus) and compared them to the full brain expression (Figure 1). *P*-values were calculated using a Kruskal–Wallis test followed by a Dunn's multiple comparisons test.

At 7 weeks, the only area that showed significantly higher levels of MeCP2 compared to full brain was the cerebellum (4.29-fold, *p*-value = 0.0002). We also screened for the expression of MeCP2 protein at 4 and 12 weeks of age, at which stage there were no significant differences between the full brain and the specific areas.

The results show that MeCP2 expression changes during development and at 7 weeks, the MeCP2 protein is highly expressed in the cerebellum.

RNA Sequencing Reveals Differentially Expressed Genes in Cerebellum and Blood of *Mecp2*-Null Mice

RNA sequencing (RNAseq) was performed on male *Mecp2*-null mice at 7 weeks of age and compared to wild-type (WT)



matched controls. The experiment was performed independently in cerebellum and blood. Tissue-dependent EdgeR analysis revealed 81 differentially expressed (DE) genes (DEGs) in cerebellum, of which 44 were upregulated and 37 downregulated (**Figure 2A**). In blood, 205 DEGs were found to be significantly different between WT and mutants: 105 upregulated and 100 downregulated. We found similar levels of gene expression in both tissues (R^2 Spearman WT = 0.95, R^2 Spearman MUT = 0.93, **Figure 2B and C**). DEGs show different profiles in the heatmaps of expression (**Figure 2D and E**). **Table 1** contains the first 10 genes of each group ordered by p -value. The full list is available in **Supplementary File 1**. As an intrinsic control, we checked the expression of *Mecp2*, and we confirmed a strong difference between WT and mutants: a log₂ fold change (log₂FC) of -3.88 in the cerebellum of *Mecp2*-null mice relative to the controls, with an FDR-corrected p -value [false discovery rate (FDR)] of $5.38E-27$. In blood, *Mecp2* showed a log₂FC of -2.50 , and an

FDR of $4.07E-06$. *Bdnf*, which is known to be downregulated in RTT, showed a log₂FC of -1.25 and an FDR of $1.05E-04$ in cerebellum, while in blood, it was not detectable.

Altogether, the comparison between blood and brain revealed high correlation of genes' expression in both tissues.

Identification of Overlapping Genes Between Cerebellum and Blood

We then proceeded to identify DEGs present in both cerebellum and blood. We found two genes with an FDR-corrected p -value < 0.05 in both tissues: *Mecp2* and *Ube2v1*. *Mecp2* showed a log₂FC of -3.88 and an FDR-corrected p -value of $5.38E-27$ in cerebellum, and a log₂FC of -2.50 and an FDR-corrected p -value of $4.07E-06$ in blood. *Ube2v1* showed a log₂FC of -2.91 and an FDR-corrected p -value of 0.02 in cerebellum, and a log₂FC of 2.58 and an FDR-corrected p -value of $4.52E-10$ in blood. These genes were selected

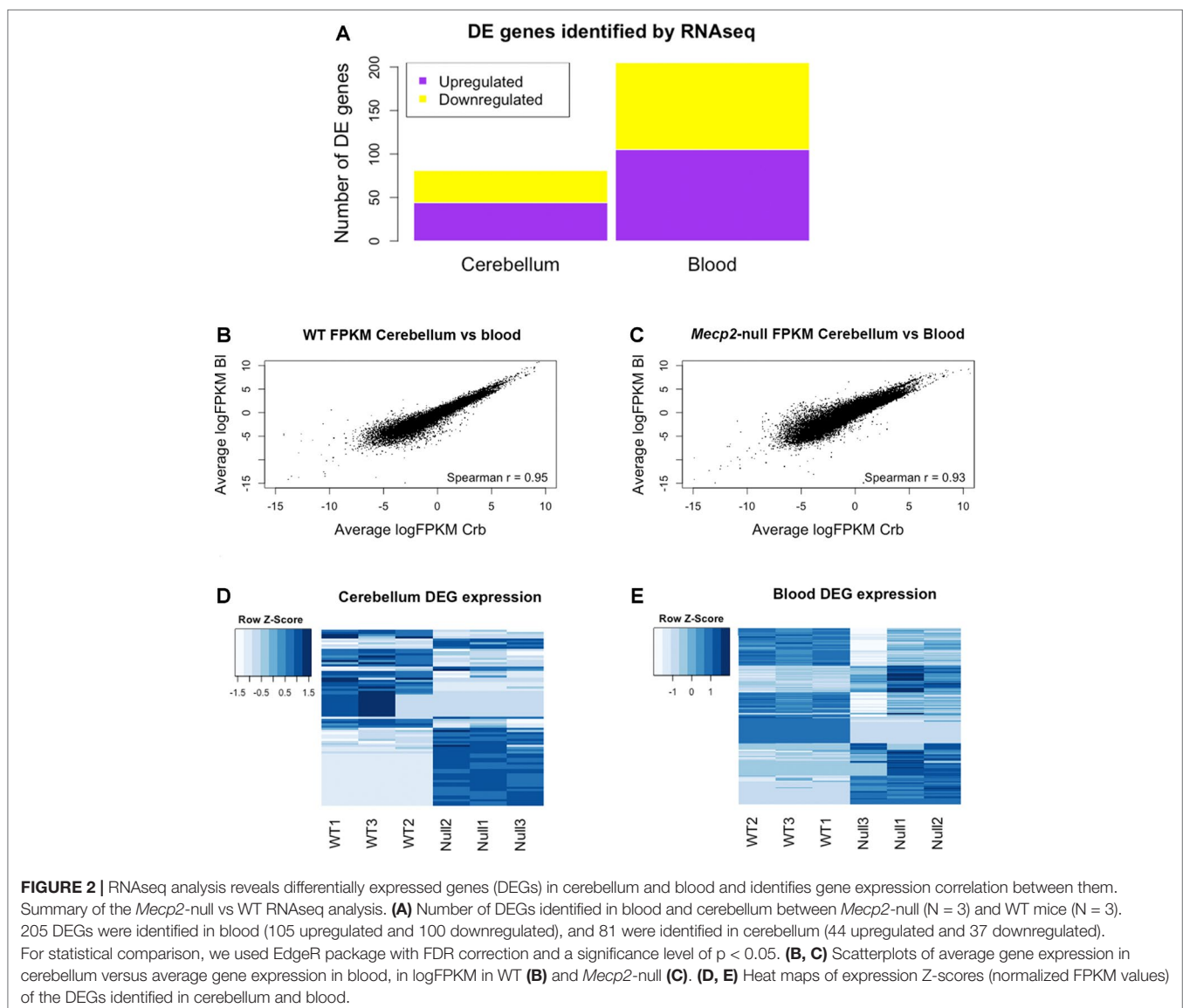


TABLE 1 | Top 10 differentially expressed genes (DEGs) ordered by *p*-value in cerebellum and blood. In both tissues, we detected a strong downregulation of *Mecp2*, which acts as a positive control of the model and the methodology. This is also the case for *Bdnf* in cerebellum. Log2CPM represents the log2-average counts per million across all samples. Log2FC represents the log2-ratio *Mecp2*-null/wild type (WT); hence, positive values mean upregulation in *Mecp2*-null and vice versa.

Gene symbol	Log2CPM	Log2FC	FDR-corrected <i>p</i> -value
Cerebellum			
<i>Mecp2</i>	6.49	-3.88	5.38E-27
<i>Gm27640</i>	0.05	6.92	1.94E-23
<i>eLsm12</i>	4.5	1.91	5.39E-19
<i>Gpr21</i>	0.06	5.22	5.09E-16
<i>Gm10408</i>	-1.41	9.60	8.96E-13
<i>Zdhhc24</i>	3.96	1.31	1.17E-06
<i>Tenm2</i>	5.53	0.99	6.32E-06
<i>Bdnf</i>	4.2	-1.25	5.29E-05
<i>Paip2</i>	7.07	1.00	1.05E-04
<i>Gm3298</i>	-3.48	7.30	2.22E-04
Blood			
<i>Ube2v1</i>	5.71	2.58	4.52E-10
<i>Bpifa1</i>	4.78	15.53	2.70E-09
<i>Tmem164</i>	3.59	3.28	4.46E-09
<i>Tnnc2</i>	0.24	10.97	6.73E-09
<i>Mmm1</i>	5.01	-3.25	4.73E-08
<i>Camp</i>	7.57	7.69	8.33E-08
<i>Scgb3a1</i>	3.88	14.63	1.75E-06
<i>Mpo</i>	4.54	10.18	1.75E-06
<i>Bace2</i>	-0.34	10.39	3.01E-06
<i>Mecp2</i>	3.85	-2.50	4.07E-06

for quantitative polymerase chain reaction (qPCR) validation with additional samples ($n = 12/\text{group}$). As expected, *Mecp2* differential expression was confirmed, with no expression in the mutant samples and average delta Ct values (dCt) of 5.31 in cerebellum and 6.26 in blood. *Ube2v1* showed significant upregulation in blood of P50 *Mecp2*-null mice (ddCt = 0.46, FC = 1.42, p -value = 0.012), and it was downregulated in cerebellum of age-matched *Mecp2*-null mice (ddCt = -0.27, FC = 0.84, p -value = 0.032), (Figure 3). An analogous comparison in presymptomatic mice showed no significant difference between mutant mice and controls (cerebellum: ddCt = 0.058, p -value = 0.354, blood: ddCt = -0.354, p -value = 0.314). Additionally, RNA quantification performed in presymptomatic females did not reveal any differences of *Ube2v1* expression between heterozygous *Mecp2*-null and WT (data not shown). All this suggests that the differential expression of *Ube2v1* is linked to the appearance of the symptoms.

Our independent validation confirmed the dysregulation of *Ube2v1* in both brain and blood, identifying a particular form of ubiquitination as a mechanism broadly altered in *Mecp2* mutants.

Gene Pathways and Network Analysis Reveals Mechanisms Dysregulated in Both Brain and Blood

To identify the cellular mechanisms differing between WT and mutant mice, we used the genes identified in the single gene analysis to perform pathway analysis, protein interaction network, and biological function analysis [gene ontology (GO)].

Potentially dysregulated pathways were identified with the iPathway software, which takes as an input differential expression data between two conditions and computes the overrepresentation and possible perturbation of biological pathways according to the differences in gene expression. The analysis revealed five significant (p -value < 0.05) pathways in cerebellum and 33 in blood. After FDR correction, the only significant pathway in cerebellum was complement and coagulation cascades and the only significant pathway in blood was platelet activation. The behavior of the complement and coagulation cascades pathway was driven by the dysregulation of the following genes: *Fga*, *Serpina1c*, and *Serpina1e*, while the affectation of the platelet activation pathway was driven by the genes: *Ptgs1*, *Mylk*, *P2rx1*, *Hpr2*, *Gp5*, *Vwf*, and *Actg1*. Interestingly, although there is no overlap between pathways in brain and blood, *Serpina1c* was identified by RNAseq to be DE both in brain and blood, so it was selected for validation with PCR (see paragraph below). The full list of genes with an uncorrected p -value < 0.05 can be found in **Supplementary File 2**.

The analysis of protein interaction network was performed with the STRINGapp in Cytoscape, which predicts interactions between the members of a protein input list, and related interactors. As input, we used the DE genes from cerebellum and blood separately. The software can identify which are the higher connected nodes in the network (“hubs”) and rank them according to the number of connections (degree).

We set up the analysis to add a maximum of 30 additional interactors per group. We then ranked the nodes by degree, in order to find proteins with the highest connectivity. In the cerebellum, the top scoring protein was Alb (Albumin), while in the blood it was Spna2 (Spectrin alpha 2). We then identified the network proteins present in both tissues, in order to find possible common mechanisms: Alb, App, Hsp90aa1, Hsp901b1, Ilt6, Kng1, Kng2, Nos1, and Spna2. Figure 4 depicts the network obtained from cerebellum, with the proteins also present in the blood analysis highlighted. The full list of proteins and their interactors, ranked by degree, can be found in **Supplementary File 3**.

The common interactors are involved in the nitric oxide biosynthesis pathway, which in STRING results statistically significant (p -value = 0.016 after FDR).

We then performed a functional enrichment analysis on the output of the STRING analysis—including both DE genes and their interactors, in order to identify overrepresented gene ontology (GO) biological process categories. The analysis of functional enrichment revealed 462 and 477 significant GO categories in cerebellum and blood, respectively. The most significantly enriched process in the cerebellum is “circadian behavior,” while in the blood it is “response to stress.” The top 10 biological processes significantly enriched in cerebellum and blood are depicted in Figure 5A and B. We found 152 overlapping significant GO biological processes between cerebellum and blood, the most significant being “response to stress.” The top 10 most significant overlapping biological processes are depicted in Figure 5C. The full list of GO categories enriched in cerebellum, blood, and their overlap can be found in **Supplementary File 4**.

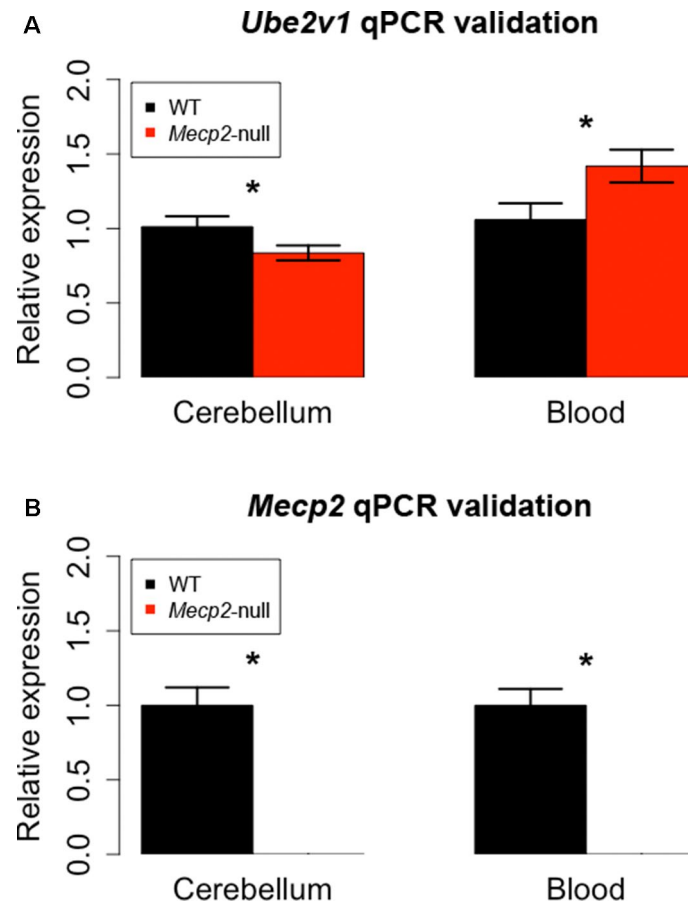


FIGURE 3 | qPCR on different biological samples validate *Ube2v1* and *Mecp2* dysregulation in brain and blood. Validation by qPCR of *Ube2v1* (A) and *Mecp2* (B) differential expression between *Mecp2*-null ($N = 6$) and WT mice ($N = 6$). Expression is represented as relative expression, calculated as $2^{-\text{ddCt}}$. Regarding *Ube2v1*, the ddCt between *Mecp2*-null and WT is 0.46 in blood (p -value = 0.012, FC = 1.42) and -0.27 in cerebellum (p -value = 0.032, FC = 0.84). In *Mecp2*-null mice, no *Mecp2* expression was detected.

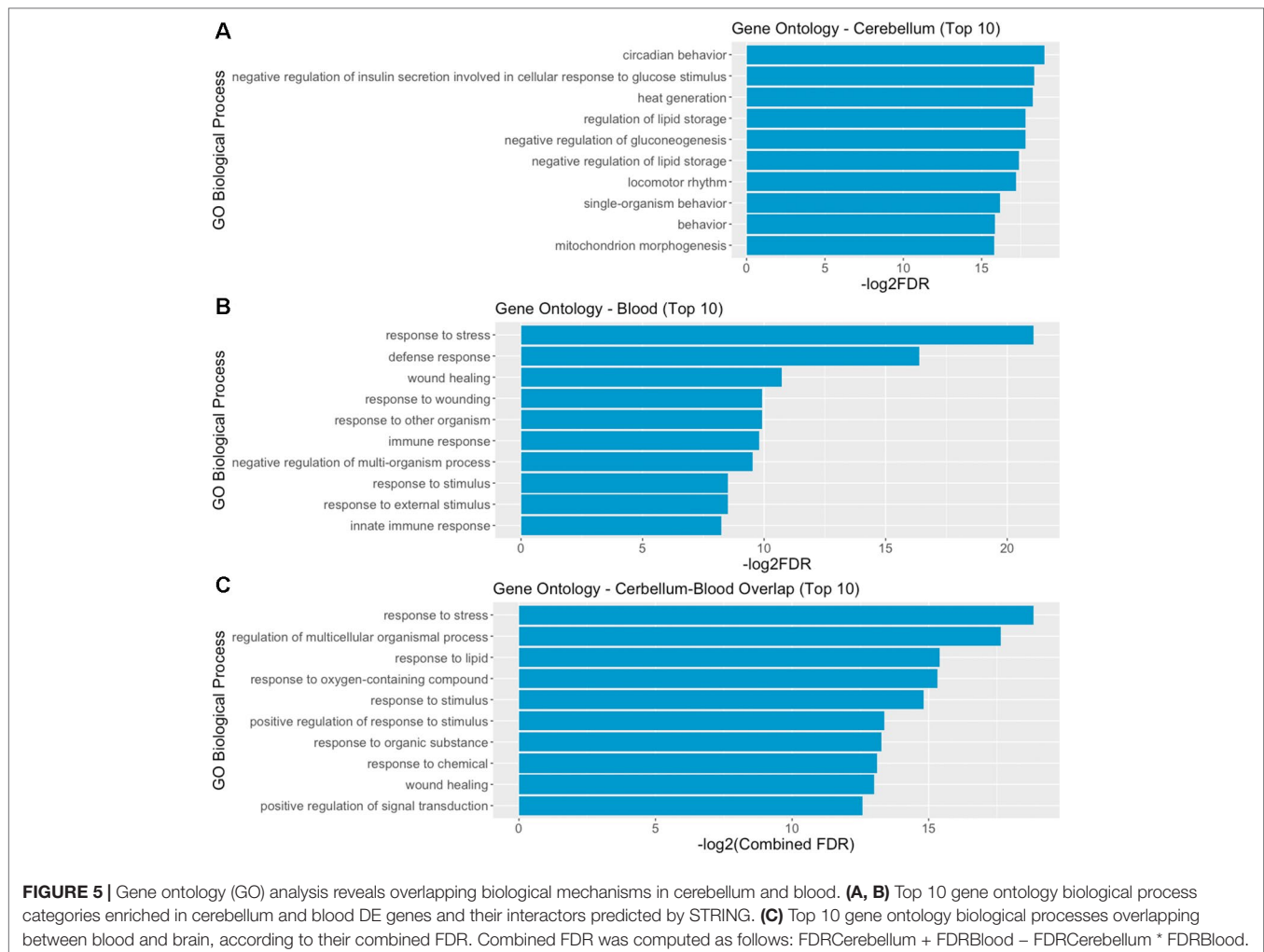
The gene-sets analysis reveals common mechanisms activated in blood and brain with an enrichment of mechanisms involved in system's homeostasis, metabolic processes such as nitric oxide synthesis, and coagulation-related processes.

qPCR Validation of Additional Genes

In addition to the identified overlapping genes in differential expression analysis, we considered for validation with qPCR additional genes that were selected according to different criteria. First, we selected genes that were significant in brain and also in blood and vice versa (Table 2). Of these, we tested with qPCR genes that were linked to the multiple gene analysis and/or were lined to mechanisms known to be associated to RTT: *Dnah14*, *Serpina1c*, *Lsm12*, *Mup10*, *Ankrd63*, *Hal*, *Ankrd63*, *Slc6a4*, *Crispld2*, *Tnnc2*, *Mpo*, *Gpx3*, *Paip2*, and *Fkbp5*. We also tested, in blood, genes that showed a high fold change or were dysregulated in cellular pathways in blood: *S100a9*, *Ms4a3*, *Snx31*, and *Prp3*, *Gstm2*, *Gsta3*, and *Itgb3*. Two of the selected genes (*Fkbp5* and *S100a9*) had already been identified

by other screenings (18). The additional tested genes are reported in Table 2.

We considered significantly different in the qPCR analysis those genes with a p -value < 0.05, and we considered "trending" the genes with a p -value between 0.1 and 0.05. The genes that confirmed to be dysregulated after qPCR are: *Serpina1c*, *Ankrd63*, *Crispld2*, *Mpo*, and *Gsta3*. The validation results are reported in Supplementary File 5. In the case of *Serpina1c*, we performed an additional PCR in liver extracts as this gene is mostly expressed by hepatocytes (19). We confirmed the downregulation of *Serpina1c* in mutants also for this preparation (ddCt = -1.006 , p -value = 0.008). We also tested the differential expression of *Serpina1c* between mutant and WT in cerebellum and blood of presymptomatic mice, obtaining negative results (cerebellum: ddCt = 1.804, p -value = 0.18, blood: ddCt = 3.563, p -value = 0.363). RNA quantification performed in presymptomatic females did not reveal any differences of *Serpina1c* expression between heterozygous *Mecp2*-null and WT (data not shown). Like in the case of *Ube2v1*, this suggests that the dysregulation of *Serpina1c* is linked to the appearance of symptoms.



not linked to proteolysis, but it acts as a system of nonproteolytic cell signaling instead (41) and has been associated to elements involved in synaptic plasticity and function. In the brain, the function of *Ube2v1* is to modulate the protein organization at synaptic level and the ability of the neurons to respond to changes in activity (**Figure 5A**). **Figure 6** represents speculations regarding possible roles of *Ube2v1* in RTT.

In a mouse study, postsynaptic density-95 (PSD95) and *Ube2v1* were copurified using tandem affinity purification (42) and *Ube2v1* mediates Lys63-linked polyubiquitination (L63-polyUb) of PSD95 in an activity-dependent and nonproteolytic manner. Such modification of PSD95 regulates two main properties associated to synaptic function: first, it affects PSD95's scaffolding properties, promoting synaptic formation, maturation, and strength (43). Second, the ubiquitination of PSD95 is known to mediate N-methyl-D-aspartate-mediated α -amino-3-hydroxy-5-methyl-4-isoxazolepropionic acid receptor (AMPA) endocytosis (44). Interestingly, the *Ube2v1* homologous *uev-1* regulates AMPAR trafficking in *Caenorhabditis elegans*, possibly by modulating a clathrin-independent AMPAR recycling pathway (45). Trafficking of AMPARs has been shown to be altered in the hippocampus

of *Mecp2*-null mice (46). There is further evidence suggesting an important function of *Ube2v1* in the brain; knocking out its associate *Ubc13* in mouse results in impaired cerebellar synapse formation (47). This hypothesis, although only theoretical, suggests that *Mecp2*, through the activity-dependent regulation of *Ube2v1*, influences L63-polyUb of PSD95. PSD95 modulates synaptic maturation and function, which indeed are impaired in RTT (48).

Outside the brain, *Ube2v1* exerts control over cell cycle and differentiation (40), response to DNA damage through p53 (49), and regulates pathways responsible for immune inflammatory response, mainly through the nuclear factor kappa-light-chain-enhancer of activated B cells (NF- κ B) pathway (50, 51) (**Figure 5B**). For instance, the UBE2V1-UBC13-TRAF6 complex activates nuclear factor of kappa light polypeptide gene enhancer in B-cells inhibitor (I κ B) kinase (IKK) in response to proinflammatory cytokines (52, 53). This mechanism is consistent with the increased levels of NF- κ B observed in MeCP2-deficient human peripheral blood mononuclear cells (PBMCs) and in the human monocyte line THP1 (54). The same authors found that the upregulation of NF- κ B caused by MeCP2 deficiency enhances the expression of tumor necrosis factor alpha (TNF α), interleukin 6 (IL-6) and interleukin 3 (IL-3)

TABLE 2 | Summary of additional genes tested by qPCR. The list includes differentially expressed (DE) genes overlapping between cerebellum and blood, some genes selected for their high fold change in blood and some genes selected from predicted dysregulated pathways. Log2FC refers to the ratio Mecp2-null/WT; hence, positive values mean upregulation in Mecp2-null and vice versa.

Additional genes tested by qPCR				
Genes identified in cerebellum that are also significant in blood				
Gene	log2FC cerebellum	FDR cerebellum	log2FC blood	Uncorrected p-value blood
<i>Dnah14</i>	2.04	2.51E-02	8.54	3.88E-03
<i>Fkbp5</i>	1.33	3.70E-02	1.40	4.90E-03
<i>Serpina1c</i>	-10.52	2.76E-02	9.87	5.50E-03
<i>Gm28374</i>	6.52	1.34E-02	-6.55	1.84E-02
<i>Lsm12</i>	1.91	5.39E-19	-1.30	3.24E-02
<i>Paip2</i>	1.00	1.06E-04	-1.06	3.49E-02
<i>Ahsa2</i>	-0.85	4.13E-02	-0.83	4.15E-02
<i>Mup10</i>	-10.75	3.30E-02	7.12	4.28E-02
Genes identified in blood that are also significant in cerebellum				
Gene	log2FC blood	FDR blood	log2FC cerebellum	Uncorrected p-value cerebellum
<i>Atp6v0d2</i>	10.74	4.30E-02	5.91	3.44E-04
<i>Hal</i>	9.73	2.87E-02	-5.88	3.65E-04
<i>Ankrd63</i>	8.90	3.79E-02	2.07	5.56E-04
<i>Hist1h2be</i>	-3.32	1.08E-02	-0.86	4.59E-03
<i>Slc6a4</i>	-1.99	2.27E-02	2.75	1.13E-02
<i>Crispld2</i>	2.54	4.87E-02	0.66	1.22E-02
<i>RP23-253114.4</i>	11.74	1.05E-02	3.12	1.28E-02
<i>C430002N11Rik</i>	-8.55	5.89E-03	4.84	1.32E-02
<i>Tnnc2</i>	10.97	6.73E-09	3.44	1.37E-02
<i>Scgb3a2</i>	14.25	2.26E-03	4.57	1.91E-02
<i>Mpo</i>	10.18	1.75E-06	1.18	2.65E-02
<i>Gm5741</i>	-8.52	9.00E-03	2.67	3.33E-02
<i>Gpx3</i>	3.03	1.64E-02	0.73	3.37E-02
High fold change in blood				
Gene	log2FC RNAseq	FDR RNAseq		
<i>S100a9</i>	2.87	2.01E-02		
<i>Srx31</i>	-8.80	3.09E-03		
<i>Ms4a3</i>	13.05	5.27E-03		
<i>Prg3</i>	12.26	5.27E-03		
Genes from predicted dysregulated pathways (blood)				
Gene	log2FC RNAseq	FDR RNAseq		
<i>Gsta3</i>	8.98	4.06E-03		
<i>Gstm2</i>	7.56	2.34E-04		
<i>Itgb3</i>	-3.15	1.00E-03		

(55), which can contribute to the subclinical immune dysregulation observed in RTT patients (56), including increased levels of TNF α and IL-6 in the blood, among other cytokines (57). Alteration of the NF- κ B pathway was also suggested after transcriptomic analysis on the blood of RTT patients (58). NF- κ B is also dysregulated in cortical neurons of *Mecp2*-null mice, with direct effects on dendritic complexity that can be rescued by reducing NF- κ B signaling (59).

The presence of *Ube2v1* across different processes and cell types, and especially in the immune system, makes it an interesting candidate to examine the function of *MECP2* in the periphery and to reflect brain function in peripheral blood. A transcriptomic analysis performed in human PBMCs revealed

enrichment of gene ontology categories related to regulation of protein ubiquitination (60). This could support the idea of *Ube2v1* also playing a role in the human condition.

Serpina1c

Serpina1c resulted to be a DEG in both blood and brain. Its downregulation in the mutants was confirmed in cerebellum and showed a strong trend in blood. In blood, the qPCR expression analysis contradicts the one originally obtained by RNAseq, which indicated a strong upregulation in the blood of mutants. The results in the sequencing analysis though, are driven by one single sample, while the results in PCR have been replicated

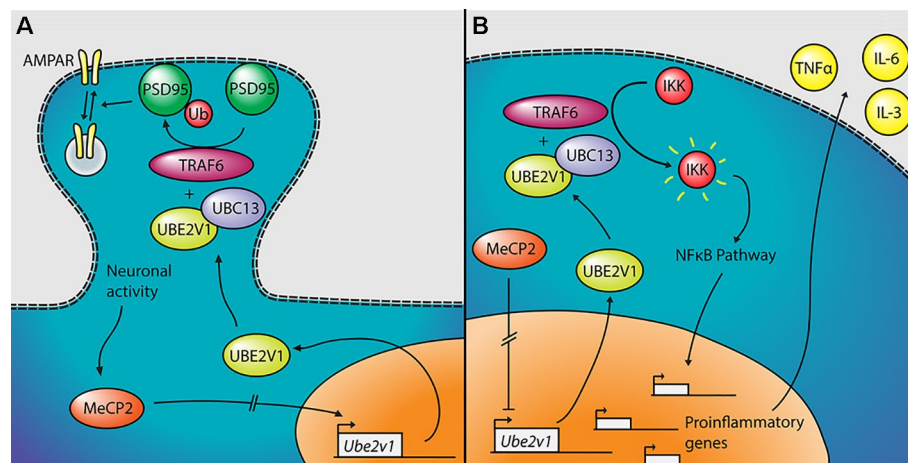


FIGURE 6 | Proposed mechanism linking *Mecp2*, *Ube2v1*, and Rett syndrome (RTT). **(A)** In neurons, MeCP2 would upregulate the transcription of *Ube2v1*, directly or indirectly. UBE2V1, together with UBC13 and TRAF6, would promote Lys63-linked ubiquitination of PSD95, which would in turn regulate AMPA receptor (AMPA) trafficking. **(B)** In peripheral blood mononuclear cells (PBMCs), MeCP2 would repress the transcription of *Ube2v1* (directly or not). UBE2V1, together with UBC13 and TRAF6, would activate IκB kinase (IKK), which would activate the NFκB pathway. This would promote the transcription of proinflammatory genes and the upregulation of cytokines such as TNFα, IL-6, and IL-3.

across 12 independent biological samples; hence, for this gene, we trust the decrease measured with PCR. The nature of *Serpina1c* gives reasons to pay attention to its possible involvement in RTT.

Serpina1c encodes for α-1-antitrypsin (α1AT) 1–3, which is part of the serine protease inhibitor (Serpin) family. While in mouse, *Serpina1* has five different variants (*Serpina1a-e*) with distinct specificity (61), in human, there is only one *SERPINA1* gene.

In mouse, the protein network for *Serpina1c* shows interactions with the elements of the Akt pathways, which has been shown to be dysregulated in *Mecp2* mutant mice (62).

In humans, mutations that result in a deficit of α1AT are mostly known to be a cause of pulmonary emphysema and liver disease (63). The liver is the main secretor of α1AT in both human and mouse, and it also expresses MeCP2. We confirmed the downregulation of *Serpina1c* RNA in the liver of mutant mice by qPCR. The MeCP2 and α1AT coexpression suggests a role of *Serpina1c/SERPINA1* in RTT.

In normal conditions, circulating α1AT protects the lungs by inhibiting neutrophil elastase, which degrades the connective tissue. Patients with low plasma levels of α1AT have an elevated risk of pulmonary emphysema, due to excessive degradation of the connective tissue. To our knowledge, respiratory deficiencies present in RTT have not been yet linked to this kind of pathology. However, emphysema-like features have been observed in the lungs of *Mecp2*-null mice (64).

The role of α1AT in liver pathogenesis would be less relevant in RTT, as its main disease-causing mechanism is the aggregation and accumulation of abnormal forms of α1AT in the hepatocytes (65, 66). The most intriguing result of the *Serpina1c* analysis is that diagnostic grade blood tests are already available to quantify the levels of circulating α1AT (67) and the same methods could be used in RTT patients for prognostic purposes.

Regarding its brain function, α1AT has been proposed to be involved in Alzheimer's disease (AD) (68), Parkinson's disease (PD) (69), schizophrenia (70), and amyotrophic lateral sclerosis (ALS) (71), but no specific mechanisms have been described. α1AT has been shown to drastically reduce excitotoxicity *in vitro* through the inhibition of calpain (72), but there is no evidence of this phenomenon being physiologically significant *in vivo*. α1AT is also therapeutic against stroke in rats (73).

It is also possible that *Serpina1c* in the brain acts through the interaction with other proteins. α1AT is an inhibitor of activated protein C (APC) (74). APC, in turn, neutralizes plasminogen activator inhibitor 1 (PAI) (75), which inhibits tissue plasminogen activator (tPA) (76). tPA is a protease that catalyzes the conversion of plasminogen to plasmin. Aside from its important anticoagulant role, plasmin is responsible for the cleavage of the inactive precursor brain derived neurotrophic factor (proBDNF) into active mature BDNF (mBDNF) (77). BDNF is considered relevant in RTT: it has been shown to be dysregulated in both RTT patients (78, 79) and in animal models (80, 81), and its overexpression in mice ameliorates the symptoms of *Mecp2*-null mice (80). MeCP2 seems to directly regulate the expression of BDNF in an activity-dependent manner (82), suggesting that the involvement of BDNF in RTT is transcription dependent. However, it is possible that the decreased expression of BDNF in RTT is dependent both by an MeCP2-dependent transcription, and by an abnormal posttranslational cleavage of BDNF. BDNF has been studied as possible peripheral biomarkers of mood disorders (83), and the tPA–BDNF pathway in serum is a target for the treatment of depression (84). Moreover, the fact that tPA's main known role is related to hemostasis would be in accordance with the dysregulation of the platelet activation mechanisms, identified with the pathways analysis.

Interestingly, RNA expression analysis of both *Ube2v1* and *Serpina1c* in presymptomatic mice shows no difference

between WT and mutant mice, suggesting that their altered expression may be linked to presentation of symptoms and severity of the condition.

Platelet Activation Pathway

Pathway analysis predicted a potential disruption of the platelet activation pathway in the blood of *Mecp2*-null mice. Interestingly, an altered coagulation pathway was identified in the brain of the same mutant mice, driven by the already discussed *Serpina1c*. If, according to the previously described hypothesis, the levels of plasmin were altered in RTT, an abnormal hemostatic state could be expected, although it has never been reported in patients.

Other mechanisms could potentially link platelet activation and RTT. In a metabolomic screening of *Mecp2*-null mice, an alteration of the platelet-activating factor (PAF) cycle was predicted (85). PAF is a multifunctional phospholipid, which acts through its G-coupled receptor PAFR (86) and is involved in activation of platelets and leucocytes and in synaptic function (87, 88).

Regarding its role in the synapse, PAF has been described as a retrograde messenger in hippocampal long-term potentiation (LTP) (89). PAF also mediates synaptic facilitation in striatal slices (90) and LTP in cortical slices (91). PAF can enhance presynaptic vesicle exocytosis through calcium signaling (92, 93). Animal models lacking PAFR have shown differing results, with a study claiming LTP attenuation (94) and another claiming a normal synaptic function (95). It has also been observed that PAF needs to be properly regulated: elevated levels of PAF can cause excitotoxicity (96), and it seems to be involved in various CNS diseases, such as AD, PD, epilepsy, stroke, or multiple sclerosis (97). LTP defects have been repeatedly observed in mouse models of RTT (46, 98–101), and PAF could be a contributing factor.

We speculate that the alteration of the platelet activation pathway could be influenced by abnormal levels of nitric oxide (described below), which has a limiting effect on platelet activation (102).

Nitric Oxide

Our protein interaction analysis revealed that some genes overlapping between blood and cerebellum could be related to the nitric oxide (NO) synthesis pathway. NO is a signaling molecule present in several biological processes. In the brain, it can act as an anterograde and retrograde neurotransmitter, and it can induce dendritic and presynaptic growth (103). As previously mentioned, synaptic function and morphology are abnormal in RTT. NO could play a role in anxiety (104)—which is characteristic of RTT (105)—and it has also been linked to other pathologies of the CNS such as schizophrenia, bipolar disorder, depression, autism, and fragile X syndrome (106, 107). Abnormal upregulation of neuronal NO synthase has been observed in enteric neurons of *Mecp2*-null mice (108). Conversely, a reduced NO availability has been observed to contribute to vascular dysfunction in *Mecp2*-null mice (109). Our data is not enough to describe if the NO levels are most likely to be up- or downregulated in our model, but it remains a hypothesis to explore further. NO would also be a potential target for a treatment. L-lysine, an inhibitor of NO synthesis, has been used in a trial as an adjuvant of risperidone in schizophrenia (110). Bumetanide, a molecule that has been shown to be effective in the treatment of ASD (111), has been

suggested to achieve its effect by increasing the levels of NO (112), but no experiments have been performed in that regard.

The analysis of enriched biological functions with GO shows consistency with other function dysregulated in RTT. The enrichment of circadian behavior in the brain preparation is consistent with sleep disorders in patients with RTT (113), and with disruption found in *Mecp2* mutant mice. *Mecp2* mutants have altered nocturnal activity and present structural abnormalities of hypothalamic centers controlling circadian rhythms (114). In addition, both MeCP2 expression and the MeCP2-binding to promoters of regulated genes are correlated to circadian rhythms (115). The altered nocturnal activity correlates with anxiety behaviors and increased plasma concentration of corticosterone—the stress hormone—linking the enrichment of circadian behavior function to the increased response to stress function, present both in brain and in blood. Other functions that appear enriched in the GO analysis of blood and brain systems include metabolism, and response to stimuli such as immune response, which have been reported to be indeed altered in patients with RTT (116, 117).

Taken together, our findings point at several genes overlapping between brain and blood and connecting the multiple aspects of RTT. These results have implications not only for the understanding of the biological mechanisms of RTT and the broad action of MeCP2 across different tissues. In fact, the presence of peripheral markers associated to brain dysfunction and linked to the symptoms of RTT, would facilitate the monitoring of the disease and the evaluation of the functional effects of candidate treatments.

METHODS

Mice

For screening the MeCP2 expression in control conditions, we used WT C57/BL6 male mice. For the sequencing experiment, we used *Mecp2*^{tm1.1Bird} male mice available from Jackson (Stock no.: 003890) with a deletion of exons 3 and 4. WT C57/BL6 male mice were used as controls, as they match the background of the mutants. For qPCR, we used additional mice from the colony. Mice were genotyped using a standard PCR on DNA extracted from ear punches, using the protocol described in the Jackson website (www.jax.org). For the selection of presymptomatic and symptomatic mice, we used the criteria defined by Stearns et al. (118), where the authors run a battery to behavioral tests to define the onset of symptoms of RTT in male mice (after 28 days after birth—P28). For female mice, the onset of symptoms is after 3 months (P90). Mice were housed in the animal facility at 12 L/D cycle. All procedures on animals were authorized by the National Authority in Animal Welfare [Health Products Regulation Authority (HPRa)] Department of Comparative Medicine in Trinity College Dublin (TCD) (Authorization number: AE1936/I108, AE1936/P067).

Protein Extraction and Enzyme-Linked Immunosorbent Assay (ELISA)

Tissue was harvested at postnatal ages of 4, 8, and 12 weeks. Cortex, hippocampus, hypothalamus, cerebellum, and full brain were dissected and stored at -80°C until protein extraction. Tissue was homogenized in radioimmunoprecipitation assay (RIPA) buffer (150 mM NaCl,

1% Triton X-100, 0.5% sodium deoxycholate, 0.1% SDS, 50 mM Tris-HCl pH = 8) containing cOmplete Protease Inhibitor Cocktail Tablets (Sigma), using pestles. The homogenate was incubated for 30 min in ice and then sonicated. The homogenate was centrifuged for 30 min at 20,000xG at 4°C, and the supernatant was stored at -80°C until further use. MeCP2 concentration was measured using a precoated sandwich ELISA assay (ELISAGENIE). The MeCP2 concentration of each sample was normalized by its total protein concentration, measured using a Pierce™ BCA Protein Assay Kit (ThermoFisher). Statistical analysis was performed using a Kruskal-Wallis nonparametric test, and results were considered significant with a *p*-value < 0.05.

RNA Extraction

Mice were sacrificed using CO₂ at 8 weeks of age. Tissue harvesting was operated between 12 and 3 PM, and littermates were used as matching controls in the majority of cases (unless matched controls were not available). All the experiments comparing mutants and WT were run simultaneously. Cerebellums were dissected and stored at -80°C until RNA extraction. Blood was extracted immediately after euthanasia by suction from the heart and stored in RNAProtect Animal Blood Tubes (Qiagen). RNA was purified from brain and blood using the miRNeasy Mini Kit (Qiagen) and the RNeasy Protect Animal Blood Kit (Qiagen), respectively. RNA purity and concentration were assessed by the A260/230 and A260/280 obtained with a NanoDrop.

RNAseq

Three *Mecp2*-null and 3 WT mice were used for RNAseq. RNA from blood was depleted from globin mRNA using a mouse/rat GLOBINclear™ kit (Ambion). RNA integrity and concentration were measured using a bioanalyzer. For the subsequent steps, only samples with an RIN (RNA Integrity Number) > 7 were used. Sequencing cDNA libraries were prepared using a NEBNext Ultra RNA Library Prep Kit for Illumina, along with a NEBNext Poly(A) mRNA Magnetic Isolation Module and the NEBNext Multiplex Oligos for Illumina (New England Biolabs). RNA (200 ng) were used as a starting material for each sample. Library concentration and mean fragment length were measured using a bioanalyzer. Libraries were pooled, and a preliminary sequencing run was performed in a MiSeq (Illumina). Then, they were sent for sequencing to Edinburgh Genomics, where a HiSeq 2000 system (Illumina) was used. Sixty million, 2x75bp paired-end reads were obtained for each sample. The quality of the reads was determined using FastQC. All reads had qualities above Q28 among their whole extent (a representative sample of the FastQC analysis is depicted in **Supplementary Figure 7**). Reads were aligned to the Ensembl GRCm38 mouse genome construct, using Hisat2 (119), with default parameters. Abundance tables were generated using Stringtie (119), using the -e and -B options (simplified protocol) and the rest of parameters on default. To obtain count tables, the output of Stringtie was processed with the prepDE.py script provided by the developers. To obtain fragments per kilobase of transcript per million mapped reads (FPKM) tables, the output of Stringtie was processed with the R package Ballgown.

The gene expression tables were filtered by removing counts corresponding to miRNA and genes presenting 0 counts in all samples. Differential expression analysis was performed using EdgeR (120), a statistical package specifically designed to analyze transcriptomic data, and we selected a likelihood ratio test. Results were corrected for multiple testing. Genes were considered as DE with an FDR-corrected *p*-value < 0.05.

Protein Interaction and Functional Enrichment Analysis

Protein interaction and functional enrichment analysis were performed in the STRINGapp plugin for Cytoscape (v.1.8.0), which uses information from the STRING database (string-db.org). DE genes obtained by RNAseq were used as an input. A maximum number of 30 maximum additional interactors was selected. The confidence score cutoff was set at 0.6. Functional enrichment analysis was also performed on Cytoscape, using the STRING Enrichment plugin.

Pathway Analysis

Pathway analysis of the results obtained by RNAseq was performed by using the iPathway software (Advaita). The software generates the *p*-value associated to each result considering the correction for multiple testing.

Identification of Common Differentially Expressed Genes in Blood and Cerebellum

Identification of the significant DEG in each tissue was performed selecting the significant genes identified by EdgeR after multiple testing correction (*P* value ≤ 0.05). For the selection of DEG in both blood and brain, we used the list of DEG in one tissue (i.e., brain) and we tested the hypothesis that they were also significant in blood with the appropriate correction. We repeated the procedure for the DEG in blood also significant in brain.

qPCR

Six *Mecp2*-null and 6 WT mice were used for qPCR. RNA was reverse transcribed using the Quantinova RT Kit (Qiagen). Reactions (20 μl) were set up, using 2x Gene Expression Master Mix (Applied Biosciences) and PrimeTime® qPCR Probe Assays (Integrated DNA Technologies). We used the following primer-probe sets:

- *S100a9*: F: GGAATTCAGACAAATGGTGAAG R: CATCA GCATCATACTACTCTCA; probe:/56-FAM/TGACATCAT/ZEN/GGAGGACCTGGACACA/3IABkFQ/
- *Ms4a3*: F: TCAATACCCAGGCTTTCAAGG R: GAGAAT CAGCATTAAGACACCAG; probe:/56-FAM/TGCAGACAT/ZEN/CAGGTGACGGTGAAG/3IABkFQ/
- *Serpina1c*: F: GGAATCACAGAGGAGAATGCT R: GAATAA GGAACGGCTAGTAAGACT; probe:/56-FAM/TGTGCATAA/ZEN/GGCTGTGCTGACCA/3IABkFQ/
- *Lsm12*: F: CCTAGCTTCACTCAATGTTAGTAAG R: ATGG TCTTGTGAATGGTCTGG; probe:/56-FAM/TCAGCTTCT/ZEN/CCTCCTTCTCCGTCC/3IABkFQ/

- *Ankrd63*: F: CCAGCTTGATTTCTTGTCT R: CCTGAG CCATCCACCTTTC; probe:/56-FAM/AGAAGCAGC/ZEN/CG TTGTTACACCT/3IABkFQ/
 - *Crispld2*: F: TCTGAGTGTCCATCCAGCTA R: TTCCA CCTCGTTCATCATATCC; probe:/56-FAM/AGAAGCAGC/ZEN/CGTTGTTACACCT/3IABkFQ/
 - *Scgb3a2*: F: CTGGTATCTATCTTTCTGCTGGTG R: GTC GTCCAAAGGTACAGGTAA; probe:/56-FAM/TGGTTATTC/ZEN/TGCCACTGCCCTTCT/3IABkFQ/
 - *Prg3*: F: CTATGTGCTGGTGAGGACTC R: AACTATA ACTGTGGACGGAAGC; probe:/56-FAM/ATCTCCTGC/ZEN/AGACTCTCTGAGCCT/3IABkFQ/
 - *Fam69c*: F: TGAGCCATTTTCGACAGTGAC R: CCATGTCTAC GTCATAGTACC; probe:/56-FAM/TGATGTCAA/ZEN/ACCT GAGAACTTCGCCA/3IABkFQ/
 - *Has2*: F: AGTCATGTACACAGCCTTCAG R: GACCTTCA CCATCTCCACAG; probe:/56-FAM/CATAATCCA/ZEN/CGCT TCGCCCCAGT/3IABkFQ/
 - *Vmn2r85*: F: CCACAGAGTCAACAACCTTCA R: GTACAT GTCACACTGCACATTG; probe:/56-FAM/ATGGGCCAC/ZEN/AGGAGGAACATCAG/3IABkFQ/
 - *Acc2os*: F: CATCCCTCTGTTGTTATTATTCATC R: TCTGC TCCACTGAGTTTACTG; probe:/56-FAM/AGCTAAGCC/ZEN/TGGTTCCTTTGTTCCCTG/3IABkFQ/
 - *Gapdh*: F: AATGGTGAAGGTCGGTGTG R: GTGGAGT CATACTGGAACATGTAG; probe:/56-FAM/TGCAAATGGCAGCC CTGGTG/3IABkFQ/
 - *Slc14a2*: F: CAACCGCATCTACTTCTGAC R: GCTC TCTTCTGCCTTCCAC; probe:/56-FAM/ACTGCTCTC/ZEN/CACTGCCACCATT/3IABkFQ/
 - *Snx31*: F: CCAGATGAGCAGAGTGAAGTG R: CTAGGTT CTGGTTGAGAGTTTCG; probe:/56-FAM/AGCAGAGTT/ZEN/CCAAGGAAAGTGACCTG/3IABkFQ/
 - *Bpifa1*: F: CCTCTCCTGAACAACATCCTC R: AGACTTCC AACTACGGGCATA; probe:/56-FAM/CCATCGTCT/ZEN/CTAT GTCACCATCCCTCT/3IABkFQ/
 - *Tfap2d*: F: TGAGCCAGGATAGATCACCA R: GCTTAGA GCTGCACATATTGC; probe:/56-FAM/CCAGACCCA/ZEN/CTCCATTCTAGACCT/3IABkFQ/
 - *Ube2v1*: F: CACTTACAAGATGGACAGGCA R: GGTACTTA GGCCCACTCTA; probe:/56-FAM/ACCTCCACG/ZEN/AAC AATCTATGAAAACCGAA/3IABkFQ/
 - *Dnah14*: F: TCAGTATAGAAGTCTCTCAGTCAR: TGCACA CGACATATTGATCCG; probe:/56-FAM/CCAGTACGA/ZEN/ACCTGACAGAATAGCTGC/3IABkFQ/
 - *Mup1*: F: TGAGAAGCATGGAATCCTTAGAG R: ATGAAC ACCAACCCACTCC; probe:/56-FAM/TATCCAATG/ZEN/CCA ATCGCTGCCTCC/3IABkFQ/
 - *Atp6v0d2*: F: AGTCTTACCTTGAGGCATTCTAC R: GCC AAATGAGTTTACAGAGTGATG; probe:/56-FAM/TCCATTCT/ZEN/TGAGTTTGAGGCCGAC/3IABkFQ/
 - *Hal*: F: CCATCAGAAATCGCAGAAAGC R: AGTTCT GTAGTGATGATGTCTTC; probe:/56-FAM/CGTACACCT/ZEN/TACGCTGCTGTCCAC/3IABkFQ/
 - *Hist1h2be*: F: CGCAAACGCTACTGAAAGGA R: TTCTTGCC GTCTTCTTCTG; probe:/56-FAM/TCTGAAGAT/ZEN/GCCT GAGCCAGCC/3IABkFQ/

- *Slc6a4*: F: CATCGTCTGTCATCTGCATCC R: CGTTGG TGTTCAGGAGTGAT; probe:/56-FAM/TCCTTAAGT/ZEN/GTCCCTGGAGTGCTGA/3IABkFQ/
 - *Tnnc2*: F: GAGTGCGGAGGAGACAAC R: CCATCAGCAT CGAACATGTCA; probe:/56-FAM/AACCATGAC/ZEN/GGACC AACAGGCT/3IABkFQ/
 - *Mpo*: F: CCCGCATTCCTTGTTTTCTG R: GCTTCTCCCC ATTCCATCG; probe:/56-FAM/CTCACCTCC/ZEN/ATGCACA CCCTCTT/3IABkFQ/
 - *Gpx3*: F: GCAGTATGCAGGCAAATATATCC R: CCCAGAAT GACCAAGCCAA; probe:/56-FAM/TCTGTGAGA/ZEN/CCTC AGTAGCTGGCT/3IABkFQ/
 - *Paip2*: F: GACAGGATTCGTTGGCTACC R: GACTTGGAT CTTTCATGGTTGG; probe:/56-FAM/TCGTTGTGCG/ZEN/TTT TTAACCCAGTGCAC/3IABkFQ/

qPCR was performed in a Quantstudio 5 Real Time PCR System (Applied Biosciences), using the following cycle: 2 min at 50°C, 10 min at 90°C, and 40x (15 s at 95°C and 1 min at 60°C). All samples were analyzed in triplicate, and *Gapdh* was used as a loading control. For target genes, we used the reporter fluorophore fluorescein amidite (FAM), and for *Gapdh*, we used Cy5. For each sample, the average *Gapdh* Ct value was subtracted from the average target Ct value, obtaining a dCt value. The average dCt of the WT group was used to calculate the ddCt value for each sample. Statistical significance was assessed using a *t*-test on the ddCt values, in Microsoft Excel. Significance was considered with a *p*-value < 0.05.

DATA AVAILABILITY STATEMENT

The datasets generated for this study can be found in the Gene Expression Omnibus, under accession number [GSE129387].

ETHICS STATEMENT

This study was carried out in accordance with the recommendations of National Animal Welfare Authority, Ireland. The protocol was approved by the Animal Ethical Committee Trinity College Dublin and HPRAs.

AUTHOR CONTRIBUTIONS

AS performed the experiments and wrote the paper; KH provided assistance in the design and analysis of the RNAseq experiment; DT contributed to sample extraction and establishment of the colony; and DT and MG designed and supervised all the parts of the research and the writing of the manuscript.

FUNDING

The study was funded by the Wellcome Trust Grant WT079408/C/06/Z issued to MG, and by an SFI FN Funded Investigator grant 208377, and an IRSF grant 207417 issued to DT.

ACKNOWLEDGMENTS

We would like to acknowledge Stephen Shovlin (Trinity College, Dublin), Emil Nguyen (Carolinska Institutet, Stockholm), and Grace d'Arcy (Trinity College, Dublin) for their assistance during the performance of experimental procedures.

REFERENCES

- Amir RE, Van Den Veyver IB, Wan M, CQ Tran, Francke U, Zoghbi HY. Rett syndrome is caused by mutations in X-linked MECP2, encoding methyl-CpG-binding protein 2. *Nat Genet* (1999) 23(october):185–8. doi: 10.1038/13810
- Chahrouh M, Zoghbi HY. The story of Rett syndrome: from clinic to neurobiology. *Neuron* (2007) 56(3):422–37. doi: 10.1016/j.neuron.2007.10.001
- Huppke P, Maier EM, Warnke A, Brendel C, Laccone F, Gärtner J. Very mild cases of Rett syndrome with skewed X inactivation. *J Med Genet* (2006) 43(10):814–6. doi: 10.1136/jmg.2006.042077
- Guy J, Hendrich B, Holmes M, Martin JE, Bird A. A mouse Mecp2-null mutation causes neurological symptoms that mimic Rett syndrome. *Nat Genet* (2001) 27(march):322–6. doi: 10.1038/85899
- Chen RZ, Akbarian S, Tudor M, Jaenisch R. Deficiency of methyl-CpG binding protein-2 in CNS neurons results in a Rett-like phenotype in mice. *Nat Genet* (2001) 27(3):327–31. doi: 10.1038/85906
- Pelka GJ, Watson CM, Radziewicz T, Hayward M, Lahooti H, Christodoulou J, et al. Mecp2 deficiency is associated with learning and cognitive deficits and altered gene activity in the hippocampal region of mice. *Brain* (2006) 129(4):887–98. doi: 10.1093/brain/awl022
- Yasui DH, Gonzales ML, Aflatooni JO, Crary FK, Hu DJ, Gavino BJ, et al. Mice with an isoform-ablating Mecp2exon 1 mutation recapitulate the neurologic deficits of Rett syndrome. *Hum Mol Genet* (2014) 23(9):2447–58. doi: 10.1093/hmg/ddu496
- Itoh M, Tahimic CGT, Ide S, Otsuki A, Sasaoka T, Noguchi S, et al. Methyl CpG-binding protein isoform MeCP2-e2 is dispensable for rett syndrome phenotypes but essential for embryo viability and placenta development. *J Biol Chem* (2012) 287(17):13859–67. doi: 10.1074/jbc.M111.309864
- Shahbazian M, Young J, Yuva-Paylor L, Spencer C, Antalffy B, Noebels J, et al. Mice with truncated MeCP2 recapitulate many Rett syndrome features and display hyperacetylation of histone H3. *Neuron* (2002) 35(2):243–54. doi: 10.1016/S0896-6273(02)00768-7
- Schaevitz LR, Gómez NB, Zhen DP, Berger-Sweeney JE. MeCP2 R168X male and female mutant mice exhibit Rett-like behavioral deficits. *Genes, Brain Behav* (2013) 12(7):732–40. doi: 10.1111/gbb.12070
- Meehan RR, Lewis JD, Bird AP. Characterization of MeCP2, a vertebrate DNA binding protein with affinity for methylated DNA. *Nucleic Acids Res* (1992) 20(19):5085–92. doi: 10.1093/nar/20.19.5085
- Chahrouh M, Jung SY, Shaw C, Zhou X, Wong STC, Qin J, et al. MeCP2, a key contributor to neurological disease, activates and represses transcription. *Science* (2008) 320(5880):1224–9. doi: 10.1126/science.1153252
- Ben-Shachar S, Chahrouh M, Thaller C, Shaw CA, Zoghbi HY. Mouse models of MeCP2 disorders share gene expression changes in the cerebellum and hypothalamus. *Hum Mol Genet* (2009) 18(13):2431–42. doi: 10.1093/hmg/ddp181
- Chen L, Chen K, Lavery LA, Baker SA, Shaw CA, Li W, et al. MeCP2 binds to non-CG methylated DNA as neurons mature, influencing transcription and the timing of onset for Rett syndrome. *Proc Natl Acad Sci* (2015) 112(17):5509–14. doi: 10.1073/pnas.1505909112
- Ross PD, Guy J, Selfridge J, Kamal B, Bahey N, Tanner E, et al. Exclusive expression of MeCP2 in the nervous system distinguishes between brain and peripheral Rett syndrome-like phenotypes HMG Advance Access. *Hum Mol Genet* (2016) 25(20):4389–404. doi: 10.1093/hmg/ddw269
- Shahbazian MD, Antalffy B, Armstrong DL, Zoghbi HY. Insight into Rett syndrome: MeCP2 levels display tissue- and cell-specific differences and correlate with neuronal maturation. *Hum Mol Genet* (2002) 11(2):115–24. doi: 10.1093/hmg/11.2.115
- Mullaney BC, Johnston MV, Blue ME. Developmental expression of methyl-CpG binding protein 2 is dynamically regulated in the rodent brain. *Neuroscience*. (2004) 123(4):939–49. doi: 10.1016/j.neuroscience.2003.11.025
- Urdinguio RG, Lopez-Serra L, Lopez-Nieva P, Alaminos M, Diaz-Uriarte R, Fernandez AF, et al. Mecp2-null mice provide new neuronal targets for rett syndrome. *PLoS One* (2008) 3(11):e3669. doi: 10.1371/journal.pone.0003669
- Yue F, Cheng Y, Breschi A, Vierstra J, Wu W, Ryba T, et al. A comparative encyclopedia of DNA elements in the mouse genome. *Nature* (2014) 515(7527):355.
- Shovlin S, Tropea D. Transcriptome level analysis in Rett syndrome using human samples from different tissues. *Orphanet J Rare Dis* (2018) 13(1):113. doi: 10.1186/s13023-018-0857-8
- Tudor M, Akbarian S, Chen RZ, Jaenisch R. Transcriptional profiling of a mouse model for Rett syndrome reveals subtle transcriptional changes in the brain. *Proc Natl Acad Sci* (2002) 99(24):15536–41. doi: 10.1073/pnas.242566899
- Nuber UA, Kriaucionis S, Roloff TC, Guy J, Selfridge J, Steinhoff C, et al. Up-regulation of glucocorticoid-regulated genes in a mouse model of Rett syndrome. *Hum Mol Genet* (2005) 14(15):2247–56. doi: 10.1093/hmg/ddi229
- Zhou Z, Hong EJEJ, Cohen S, Zhao W, Ho HH, Schmidt L, et al. Brain-specific phosphorylation of MeCP2 regulates activity-dependent Bdnf transcription, dendritic growth, and spine maturation. *Neuron* (2006) 52(2):255–69. doi: 10.1016/j.neuron.2006.09.037
- Jordan C, Li HH, Kwan HC, Francke U. Cerebellar gene expression profiles of mouse models for Rett syndrome reveal novel MeCP2 targets. *BMC Med Genet*. (2007) 8:36. doi: 10.1186/1471-2350-8-36
- Wu H, Tao J, Chen PJ, Shahab A, Ge W, Hart RP, et al. Genome-wide analysis reveals methyl-CpG-binding protein 2-dependent regulation of microRNAs in a mouse model of Rett syndrome. *Proc Natl Acad Sci U S A* (2010) 107(42):18161–6. doi: 10.1073/pnas.1005595107
- Roux JC, Zala D, Panayotis N, Borges-Correia A, Saudou F, Villard L. Modification of Mecp2 dosage alters axonal transport through the Huntingtin/Hap1 pathway. *Neurobiol Dis* (2012) 45(2):786–95. doi: 10.1016/j.nbd.2011.11.002
- Großer E, Hirt U, Janc OA, Menzfeld C, Fischer M, Kempkes B, et al. Oxidative burden and mitochondrial dysfunction in a mouse model of Rett syndrome. *Neurobiol Dis* (2012) 48(1):102–14. doi: 10.1016/j.nbd.2012.06.007
- Samaco RC, Mandel-Brehm C, McGraw CM, Shaw CA, McGill BE, Zoghbi HY. Crh and Oprm1 mediate anxiety-related behavior and social approach in a mouse model of MECP2 duplication syndrome. *Nat Genet* (2012) 44(2):206–11. doi: 10.1038/ng.1066
- Petazzi P, Sandoval J, Szczesna K, Jorge OC, Roa L, Sayols S, et al. Dysregulation of the long non-coding RNA transcriptome in a Rett syndrome mouse model. *RNA Biol* (2013) 10(7):1197–203. doi: 10.4161/rna.24286
- Zhao YT, Goffin D, Johnson BS, Zhou Z. Loss of MeCP2 function is associated with distinct gene expression changes in the striatum. *Neurobiol Dis* (2013) 59:257–66. doi: 10.1016/j.nbd.2013.08.001
- Baker SA, Chen L, Wilkins AD, Yu P, Lichtarge O, Zoghbi HY. An AT-hook domain in MeCP2 determines the clinical course of Rett syndrome and related disorders. *Cell* (2013) 152(5):984–96. doi: 10.1016/j.cell.2013.01.038
- Sugino K, Hempel CM, Okaty BW, Arnsen HA, Kato S, Dani VS, et al. Cell-type-specific repression by methyl-CpG-binding protein 2 is biased toward long genes. *J Neurosci* (2014) 34(38):12877–83. doi: 10.1523/JNEUROSCI.2674-14.2014
- Gabel HW, Kinde B, Stroud H, Gilbert CS, Harmin DA, Kastan NR, et al. Disruption of DNA-methylation-dependent long gene repression in Rett syndrome. *Nature* (2015) 522(7554):89–93. doi: 10.1038/nature14319

SUPPLEMENTARY MATERIAL

The Supplementary Material for this article can be found online at: <https://www.frontiersin.org/articles/10.3389/fpsy.2019.00278/full#supplementary-material>

34. Li R, Dong Q, Yuan X, Zeng X, Gao Y, Chiao C, et al. Misregulation of alternative splicing in a mouse model of Rett syndrome. *PLoS Genet* (2016) 12(6):e1006129. doi: 10.1371/journal.pgen.1006129
35. Pacheco NL, Heaven MR, Holt LM, Crossman DK, Boggio KJ, Shaffer SA, et al. RNA sequencing and proteomics approaches reveal novel deficits in the cortex of Mecp2-deficient mice, a model for Rett syndrome. *Mol Autism* (2017) 8:56. doi: 10.1186/s13229-017-0174-4
36. Johnson BS, Zhao YT, Fasolino M, Lamonica JM, Kim YJ, Georgakilas G, et al. Biotin tagging of Mecp2 in mice reveals contextual insights into the Rett syndrome transcriptome. *Nat Med* (2017) 23(10):1203–14. doi: 10.1038/nm.4406
37. Zhao D, Mokhtari R, Pedrosa E, Birnbaum R, Zheng D, Lachman HM. Transcriptome analysis of microglia in a mouse model of Rett syndrome: differential expression of genes associated with microglia/macrophage activation and cellular stress. *Mol Autism* (2017) 8(1):17. doi: 10.1186/s13229-017-0134-z
38. Osenberg S, Karten A, Sun J, Li J, Charkowick S, Felice CA, et al. Activity-dependent aberrations in gene expression and alternative splicing in a mouse model of Rett syndrome. *Proc Natl Acad Sci U S A* (2018) 115(23):201722546. doi: 10.1073/pnas.1722546115
39. Gulmez Karaca K, Brito DVC, Zeuch B, Oliveira AMM. Adult hippocampal Mecp2 preserves the genomic responsiveness to learning required for long-term memory formation. *Neurobiol Learn Mem* (2018) 149:84–97. doi: 10.1016/j.nlm.2018.02.010
40. Sancho E, Vilá MR, Sánchez-Pulido L, Lozano JJ, Paciucci R, Nadal M, et al. Role of UEV-1, an inactive variant of the E2 ubiquitin-conjugating enzymes, in *in vitro* differentiation and cell cycle behavior of HT-29-M6 intestinal mucosecretory cells. *Mol Cell Biol* (1998) 18(1):576–89. doi: 10.1128/MCB.18.1.576
41. Chen ZJ, Sun LJ. Nonproteolytic functions of ubiquitin in cell signaling. *Mol Cell* (2009) 33(3):275–86. doi: 10.1016/j.molcel.2009.01.014
42. Fernández E, Collins MO, Uren RT, Kopanitsa MV, Komiya NH, Croning MD, et al. Targeted tandem affinity purification of PSD-95 recovers core postsynaptic complexes and schizophrenia susceptibility proteins. *Mol Syst Biol* (2009) 5:269. doi: 10.1038/msb.2009.27
43. Ma Q, Ruan H, Peng L, Zhang M, Gack MU, Yao W-D. Proteasome-independent polyubiquitin linkage regulates synapse scaffolding, efficacy, and plasticity. *Proc Natl Acad Sci U S A* (2017) 114(41):E8760–9. doi: 10.1073/pnas.1620153114
44. Colledge M, Snyder EM, Crozier RA, Soderling JA, Jin Y, Langeberg LK, et al. Ubiquitination regulates PSD-95 degradation and AMPA receptor surface expression. *Neuron* (2003) 40(3):595–607. doi: 10.1016/S0896-6273(03)00687-1
45. Kramer LB, Shim J, Previtera ML, Isack NR, Lee M-C, Firestein BL, et al. UEV-1 is an ubiquitin-conjugating enzyme variant that regulates glutamate receptor trafficking in *C. elegans* neurons. *PLoS One* (2010) 5(12):e14291. doi: 10.1371/journal.pone.0014291
46. Li W, Xu X, Pozzo-Miller L. Excitatory synapses are stronger in the hippocampus of Rett syndrome mice due to altered synaptic trafficking of AMPA-type glutamate receptors. *Proc Natl Acad Sci U S A* (2016) 113(11):E1575–84. doi: 10.1073/pnas.1517244113
47. Valnegri P, Huang J, Yamada T, Yang Y, Mejia LA, Cho HY, et al. RNF8/UBC13 ubiquitin signaling suppresses synapse formation in the mammalian brain. *Nat Commun* (2017) 8(1):1271. doi: 10.1038/s41467-017-01333-6
48. Feldman D, Banerjee A, Sur M. Developmental dynamics of rett syndrome. *Neural Plast* (2016) 2016:6154080. doi: 10.1155/2016/6154080
49. Laine A, Topisirovic I, Zhai D, Reed JC, Borden KLB, Ronai Z. Regulation of p53 localization and activity by Ubc13. *Mol Cell Biol* (2006) 26(23):8901–13. doi: 10.1128/MCB.01156-06
50. Hodge CD, Spyrapoulos L, Glover JNM. Ubc13: the Lys63 ubiquitin chain building machine. *Oncotarget* (2016) 7(39):64471–504. doi: 10.18632/oncotarget.10948
51. Wu X, Karin M. Emerging roles of Lys63-linked polyubiquitylation in immune responses. *Immunol Rev* (2015) 266(1):161–74. doi: 10.1111/imr.12310
52. Deng L, Wang C, Spencer E, Yang L, Braun A, You J, et al. Activation of the IkappaB kinase complex by TRAF6 requires a dimeric ubiquitin-conjugating enzyme complex and a unique polyubiquitin chain. *Cell* (2000) 103(2):351–61. doi: 10.1016/S0092-8674(00)00126-4
53. Wang C, Deng L, Hong M, Akkaraju GR, Inoue J, Chen ZJ. TAK1 is a ubiquitin-dependent kinase of MKK and IKK. *Nature* (2001) 412(6844):346–51. doi: 10.1038/35085597
54. O'Driscoll CM, Kaufmann WE, Bressler JP. Mecp2 deficiency enhances glutamate release through NF-κB signaling in myeloid derived cells. *J Neuroimmunol* (2013) 265(1–2):61–7. doi: 10.1016/j.jneuroim.2013.09.002
55. O'Driscoll CM, Lima MP, Kaufmann WE, Bressler JP. Methyl CpG binding protein 2 deficiency enhances expression of inflammatory cytokines by sustaining NF-κB signaling in myeloid derived cells. *J Neuroimmunol* (2015) 283:23–9. doi: 10.1016/j.jneuroim.2015.04.005
56. Cortelazzo A, De Felice C, Guerranti R, Signorini C, Leoncini S, Pecorelli A, et al. Subclinical inflammatory status in Rett syndrome. *Mediators Inflamm* (2014) 2014:480980. doi: 10.1155/2014/480980
57. Leoncini S, De Felice C, Signorini C, Zollo G, Cortelazzo A, Durand T, et al. Cytokine dysregulation in MECP2- and CDKL5-related Rett syndrome: relationships with aberrant redox homeostasis, inflammation, and ω-3 PUFAs. *Oxid Med Cell Longev* (2015) 2015:421624. doi: 10.1155/2015/421624
58. Colak D, Al-Dhalaan H, Nester M, AlBakheet A, Al-Younes B, Al-Hassnan Z, et al. Genomic and transcriptomic analyses distinguish classic Rett and Rett-like syndrome and reveals shared altered pathways. *Genomics* (2011) 97(1):19–28. doi: 10.1016/j.ygeno.2010.09.004
59. Kishi N, MacDonald JL, Ye J, Molyneaux BJ, Azim E, Macklis JD. Reduction of aberrant NF-κB signalling ameliorates Rett syndrome phenotypes in Mecp2-null mice. *Nat Commun* (2016) 7:10520. doi: 10.1038/ncomms10520
60. Pecorelli A, Leoni G, Cervellati F, Canali R, Signorini C, Leoncini S, et al. Genes related to mitochondrial functions, protein degradation, and chromatin folding are differentially expressed in lymphomonocytes of Rett syndrome patients. *Mediators Inflamm* (2013) 2013:137629. doi: 10.1155/2013/137629
61. Paterson T, Moore S. The expression and characterization of five recombinant murine α1-protease inhibitor proteins. *Biochem Biophys Res Commun* (1996) 219(1):64–9. doi: 10.1006/bbrc.1996.0182
62. Tropea D, Giacometti E, Wilson NR, Beard C, McCurry C, Fu DD, et al. Partial reversal of Rett syndrome-like symptoms in Mecp2 mutant mice. *Proc Natl Acad Sci U S A* (2009) 106(6):2029–34. doi: 10.1073/pnas.0812394106
63. Janciauskiene SM, Bals R, Koczulla R, Vogelmeier C, Köhnlein T, Welte T. The discovery of α1-antitrypsin and its role in health and disease. *Respir Med* (2011) 105(8):1129–39. doi: 10.1016/j.rmed.2011.02.002
64. Kida H, Takahashi T, Nakamura Y, Kinoshita T, Hara M, Okamoto M, et al. Pathogenesis of lethal aspiration pneumonia in Mecp2-null mouse model for Rett syndrome. *Sci Rep* (2017) 7(1):12032. doi: 10.1038/s41598-017-12293-8
65. Lomas DA, Li-Evans D, Finch JT, Carrell RW. The mechanism of Z α1-antitrypsin accumulation in the liver. *Nature* (1992) 357(6379):605–7. doi: 10.1038/357605a0
66. Ekeowa UI, Freeke J, Miranda E, Gooptu B, Bush MF, Pérez J, et al. Defining the mechanism of polymerization in the serpinopathies. *Proc Natl Acad Sci U S A* (2010) 107(40):17146–51. doi: 10.1073/pnas.1004785107
67. American Thoracic Society, European Respiratory Society. American Thoracic Society/European Respiratory Society statement. *Am J Respir Crit Care Med* (2003) 168(7):818–900. doi: 10.1164/rccm.168.7.818
68. Song F, Poljak A, Smythe GA, Sachdev P. Plasma biomarkers for mild cognitive impairment and Alzheimer's disease. *Brain Res Rev* (2009) 61(2):69–80. doi: 10.1016/j.brainresrev.2009.05.003
69. Jesse S, Lehnert S, Jahn O, Parnetti L, Soininen H, Herukka S-K, et al. Differential sialylation of serpin A1 in the early diagnosis of Parkinson's disease dementia. *PLoS One* (2012) 7(11):e48783. doi: 10.1371/journal.pone.0048783
70. Chan MK, Cooper JD, Heilmann-Heimbach S, Frank J, Witt SH, Nöthen MM, et al. Associations between SNPs and immune-related circulating proteins in schizophrenia. *Sci Rep* (2017) 7(1):12586. doi: 10.1038/s41598-017-12986-0
71. Ebbert MTW, Ross CA, Prgent LJ, Lank RJ, Zhang C, Katzman RB, et al. Conserved DNA methylation combined with differential frontal cortex and cerebellar expression distinguishes C9orf72-associated and sporadic ALS, and implicates SERPINA1 in disease. *Acta Neuropathol* (2017) 134(5):715–28. doi: 10.1007/s00401-017-1760-4
72. Gold M, Koczulla A-R, Mengel D, Koepke J, Dodel R, Dontcheva G, et al. Reduction of glutamate-induced excitotoxicity in murine primary neurons involving calpain inhibition. *J Neurol Sci* (2015) 359(1–2):356–62. doi: 10.1016/j.jns.2015.11.016

73. Moldthan HL, Hirko AC, Thinschmidt JS, Grant MB, Li Z, Peris J, et al. Alpha 1-antitrypsin therapy mitigated ischemic stroke damage in rats. *J Stroke Cerebrovasc Dis* (2014) 23(5):e355–63. doi: 10.1016/j.jstrokecerebrovasdis.2013.12.029
74. Heeb MJ, Griffin JH. Physiologic inhibition of human activated protein C by alpha 1-antitrypsin. *J Biol Chem* (1988) 263(24):11613–6.
75. de Fouw NJ, de Jong YF, Haverkate F, Bertina RM. Activated protein C increases fibrin clot lysis by neutralization of plasminogen activator inhibitor—no evidence for a cofactor role of protein S. *Thromb Haemost* (1988) 60(2):328–33. doi: 10.1055/s-0038-1647055
76. Sprengers E, Kluff C. Plasminogen activator inhibitors. *Blood* (1987) 69(2):381–7.
77. Pang PT, Teng HK, Zaitsev E, Woo NT, Sakata K, Zhen S, et al. Cleavage of proBDNF by tPA/plasmin is essential for long-term hippocampal plasticity. *Science* (2004) 306(5695):487–91. doi: 10.1126/science.1100135
78. Abuhatzira L, Makedonski K, Kaufman Y, Razin A, Shemer R. MeCP2 deficiency in the brain decreases BDNF levels by REST/CoREST-mediated repression and increases TRKB production. *Epigenetics* (2007) 2(4):214–22. doi: 10.1016/j.epi.2.4.5212
79. Deng V, Matagne V, Banine F, Frerking M, Ohliger P, Budden S, et al. FXYD1 is an MeCP2 target gene overexpressed in the brains of Rett syndrome patients and Mecp2-null mice. *Hum Mol Genet* (2007) 16(6):640–50. doi: 10.1093/hmg/ddm007
80. Chang Q, Khare G, Dani V, Nelson S, Jaenisch R. The disease progression of Mecp2 mutant mice is affected by the level of BDNF expression. *Neuron* (2006) 49(3):341–8. doi: 10.1016/j.neuron.2005.12.027
81. Wang H, Chan S, Ogier M, Hellard D, Wang Q, Smith C, et al. Dysregulation of brain-derived neurotrophic factor expression and neurosecretory function in Mecp2 null mice. *J Neurosci* (2006) 26(42):10911–5. doi: 10.1523/JNEUROSCI.1810-06.2006
82. Klose RJ, Sarraf SA, Schmiedeberg L, McDermott SM, Stancheva I, Bird AP. DNA binding selectivity of MeCP2 due to a requirement for A/T sequences adjacent to methyl-CpG. *Mol Cell* (2005) 19(5):667–78. doi: 10.1016/j.molcel.2005.07.021
83. Hashimoto K. Brain-derived neurotrophic factor as a biomarker for mood disorders: an historical overview and future directions. *Psychiatry Clin Neurosci* (2010) 64(4):341–57. doi: 10.1111/j.1440-1819.2010.02113.x
84. Jiang H, Chen S, Li C, Lu N, Yue Y, Yin Y, et al. The serum protein levels of the tPA-BDNF pathway are implicated in depression and antidepressant treatment. *Transl Psychiatry* (2017) 7(4):e1079. doi: 10.1038/tp.2017.43
85. Viola A, Saywell V, Villard L, Cozzone PJ, Lutz NW. Metabolic fingerprints of altered brain growth, osmoregulation and neurotransmission in a Rett syndrome model. *PLoS One* (2007) 2(1):e157. doi: 10.1371/journal.pone.0000157
86. Nakamura M, Honda Z, Izumi T, Sakanaka C, Mutoh H, Minami M, et al. Molecular cloning and expression of platelet-activating factor receptor from human leukocytes. *J Biol Chem* (1991) 266(30):20400–5.
87. Prescott SM, Zimmerman GA, Stafforini DM, McIntyre TM. Platelet-activating factor and related lipid mediators. *Annu Rev Biochem* (2000) 69(1):419–45. doi: 10.1146/annurev.biochem.69.1.419
88. Bazan NG. Synaptic lipid signaling: significance of polyunsaturated fatty acids and platelet-activating factor. *J Lipid Res* (2003) 44(12):2221–33. doi: 10.1194/jlr.R300013-JLR200
89. Kato K, Clark GD, Bazan NG, Zorumski CF. Platelet-activating factor as a potential retrograde messenger in CA1 hippocampal long-term potentiation. *Nature* (1994) 367(13):175–9. doi: 10.1038/367175a0
90. Lu S-M, Tong N, Gelbard HA. The phospholipid mediator platelet-activating factor mediates striatal synaptic facilitation. *J Neuroimmune Pharmacol* (2007) 2(2):194–201. doi: 10.1007/s11481-007-9064-4
91. Heusler P, Boehmer G. Platelet-activating factor contributes to the induction of long-term potentiation in the rat somatosensory cortex *in vitro*. *Brain Res* (2007) 1135(1):85–91. doi: 10.1016/j.brainres.2006.12.016
92. Moriguchi S, Shioda N, Yamamoto Y, Fukunaga K. Platelet-activating factor-induced synaptic facilitation is associated with increased calcium/calmodulin-dependent protein kinase II, protein kinase C and extracellular signal-regulated kinase activities in the rat hippocampal CA1 region. *Neuroscience* (2010) 166(4):1158–66. doi: 10.1016/j.neuroscience.2010.01.008
93. Hammond JW, Lu S-M, Gelbard HA. Platelet activating factor enhances synaptic vesicle exocytosis *via* PKC, elevated intracellular calcium, and modulation of synapsin 1 dynamics and phosphorylation. *Front Cell Neurosci* (2015) 9:505. doi: 10.3389/fncel.2015.00505
94. Chen C, Magee JC, Marcheselli V, Hardy M, Bazan NG. Attenuated LTP in hippocampal dentate gyrus neurons of mice deficient in the PAF receptor. *J Neurophysiol* (2001) 85(1):384–90. doi: 10.1152/jn.2001.85.1.384
95. Kobayashi K, Ishii S, Kume K, Takahashi T, Shimizu T, Manabe T. Platelet-activating factor receptor is not required for long-term potentiation in the hippocampal CA1 region. *Eur J Neurosci* (1999) 11(4):1313–6. doi: 10.1046/j.1460-9568.1999.00538.x
96. Bellizzi MJ, Lu S-M, Masliah E, Gelbard HA. Synaptic activity becomes excitotoxic in neurons exposed to elevated levels of platelet-activating factor. *J Clin Invest* (2005) 115(11):3185–92. doi: 10.1172/JCI25444
97. Liu Y, Shields LBE, Gao Z, Wang Y, Zhang YP, Chu T, et al. Current understanding of platelet-activating factor signaling in central nervous system diseases. *Mol Neurobiol* (2017) 54(7):5563–72. doi: 10.1007/s12035-016-0062-5
98. Moretti P, Levenson JM, Battaglia F, Atkinson R, Teague R, Antalffy B, et al. Learning and memory and synaptic plasticity are impaired in a mouse model of Rett syndrome. *J Neurosci* (2006) 26(1):319–27. doi: 10.1523/JNEUROSCI.2623-05.2006
99. Weng S-M, McLeod F, Bailey MES, Cobb SR. Synaptic plasticity deficits in an experimental model of rett syndrome: long-term potentiation saturation and its pharmacological reversal. *Neuroscience* (2011) 180:314–21. doi: 10.1016/j.neuroscience.2011.01.061
100. Balakrishnan S, Niebert M, Richter DW. Rescue of cyclic AMP mediated long term potentiation impairment in the hippocampus of Mecp2 knockout (Mecp2-*ly*) mice by rolipram. *Front Cell Neurosci* (2016) 10:15. doi: 10.3389/fncel.2016.00015
101. Li W, Bellot-Saez A, Phillips ML, Yang T, Longo FM, Pozzo-Miller L. A small-molecule TrkB ligand restores hippocampal synaptic plasticity and object location memory in Rett syndrome mice. *Dis Model Mech* (2017) 10(7):837–45. doi: 10.1242/dmm.029959
102. van Hinsbergh VWM. Endothelium—role in regulation of coagulation and inflammation. *Semin Immunopathol* (2012) 34(1):93–106. doi: 10.1007/s00281-011-0285-5
103. Picón-Pagès P, Garcia-Buendia J, Muñoz FJ. Functions and dysfunctions of nitric oxide in brain. *Biochim Biophys Acta - Mol Basis Dis* (2018) S0925–4439(18):30452–6. doi: 10.1016/j.bbadis.2018.11.007
104. Gulati K, Rai N, Ray A. Nitric oxide and anxiety. *Vitam Horm* (2017) 169–92. doi: 10.1016/bs.vh.2016.09.001
105. Barnes KV, Coughlin FR, O’Leary HM, Bruck N, Bazin GA, Beinecke EB, et al. Anxiety-like behavior in Rett syndrome: characteristics and assessment by anxiety scales. *J Neurodev Disord* (2015) 7(1):30. doi: 10.1186/s11689-015-9127-4
106. Akyol O, Zoroglu SS, Armutcu F, Sahin S, Gurel A. Nitric oxide as a physiopathological factor in neuropsychiatric disorders. *In Vivo* (2004) 18(3):377–90.
107. Colvin SM, Kwan KY. Dysregulated nitric oxide signaling as a candidate mechanism of fragile X syndrome and other neuropsychiatric disorders. *Front Genet* (2014) 5:239. doi: 10.3389/fgene.2014.00239
108. Wahba G, Schock SC, Cudd S, Grynspan D, Humphreys P, Staines WA. Activity and MeCP2-dependent regulation of nNOS levels in enteric neurons. *Neurogastroenterol Motil* (2016) 28(11):1723–30. doi: 10.1111/nmo.12873
109. Panighini A, Duranti E, Santini F, Maffei M, Pizzorusso T, Funel N, et al. Vascular dysfunction in a mouse model of Rett syndrome and effects of curcumin treatment. *PLoS One* (2013) 8(5):e64863. doi: 10.1371/journal.pone.0064863
110. Zeinoddini A, Ahadi M, Farokhnia M, Rezaei F, Tabrizi M, Akhondzadeh S. L-lysine as an adjunct to risperidone in patients with chronic schizophrenia: a double-blind, placebo-controlled, randomized trial. *J Psychiatr Res* (2014) 59:125–31. doi: 10.1016/j.jpsychires.2014.08.016
111. Du L, Shan L, Wang B, Li H, Xu Z, Staal WG, et al. A pilot study on the combination of applied behavior analysis and bumetanide treatment for children with autism. *J Child Adolesc Psychopharmacol* (2015) 25(7):585–8. doi: 10.1089/cap.2015.0045

112. Fluegge K. Bumetanide treatment for psychiatric disorders and the modulation of central nitric oxide metabolism. *Clin Neuropharmacol* (2017) 40(4):192–3. doi: 10.1097/WNF.0000000000000228
113. Young D, Nagarajan L, de Klerk N, Jacoby P, Ellaway C, Leonard H. Sleep problems in Rett syndrome. *Brain Dev* (2007) 29(10):609–16. doi: 10.1016/j.braindev.2007.04.001
114. Li Q, Loh DH, Kudo T, Truong D, Derakhshesh M, Kaswan ZM, et al. Circadian rhythm disruption in a mouse model of Rett syndrome circadian disruption in RTT. *Neurobiol Dis* (2015) 77:155–64. doi: 10.1016/j.nbd.2015.03.009
115. Martínez de Paz A, Sanchez-Mut JV, Samitier-Martí M, Petazzi P, Sáez M, Szczesna K, et al. Circadian cycle-dependent MeCP2 and brain chromatin changes. *PLoS One* (2015) 10(4):e0123693. doi: 10.1371/journal.pone.0123693
116. Papini AM, Nuti F, Real-Fernandez F, Rossi G, Tiberi C, Sabatino G, et al. Immune dysfunction in Rett syndrome patients revealed by high levels of serum anti-N(Glc) IgM antibody fraction. *J Immunol Res* (2014) 2014:260973. doi: 10.1155/2014/260973
117. Kyle SM, Vashi N, Justice MJ. Rett syndrome: a neurological disorder with metabolic components. *Open Biol* (2018) 8(2):170216. doi: 10.1098/rsob.170216
118. Stearns NA, Schaevitz LR, Bowling H, Nag N, Berger UV, Berger-Sweeney J. Behavioral and anatomical abnormalities in Mecp2 mutant mice: a model for Rett syndrome. *Neuroscience* (2007 May 25);146(3):907–21.
119. Pertea M, Kim D, Pertea GM, Leek JT, Salzberg SL. Transcript-level expression analysis of RNA-seq experiments with HISAT, StringTie and Ballgown. *Nat Protoc* (2016) 11(9):1650–67. doi: 10.1038/nprot.2016.095
120. Robinson MD, McCarthy DJ, Smyth GK. edgeR: a bioconductor package for differential expression analysis of digital gene expression data. *Bioinformatics* (2010) 26(1):139–40. doi: 10.1093/bioinformatics/btp616

Conflict of Interest Statement: The authors declare that the research was conducted in the absence of any commercial or financial relationships that could be construed as a potential conflict of interest.

Copyright © 2019 Sanfeliu, Hokamp, Gill and Tropea. This is an open-access article distributed under the terms of the Creative Commons Attribution License (CC BY). The use, distribution or reproduction in other forums is permitted, provided the original author(s) and the copyright owner(s) are credited and that the original publication in this journal is cited, in accordance with accepted academic practice. No use, distribution or reproduction is permitted which does not comply with these terms.